

*Exhibit #2*

## Fire Detection for Conveyor Belt Entries

By Charles D. Litton, Charles P. Lazzara,  
and Frank J. Perzak

RECEIVED Office of  
Standards, Regs,  
and Variances  
2003 JUN 30 PM 4:43  
MSHA  
U.S. Dept of Labor

UNITED STATES DEPARTMENT OF THE INTERIOR



BUREAU OF MINES

Mission: As the Nation's principal conservation agency, the Department of the Interior has responsibility for most of our nationally-owned public lands and natural and cultural resources. This includes fostering wise use of our land and water resources, protecting our fish and wildlife, preserving the environmental and cultural values of our national parks and historical places, and providing for the enjoyment of life through outdoor recreation. The Department assesses our energy and mineral resources and works *to* assure that their development is in the best interests of all our people. The Department also promotes the goals of the Take Pride in America campaign by encouraging stewardship and citizen responsibility for the public lands and promoting citizen participation in their care. The Department also has a major responsibility for American Indian reservation communities and for people who live in Island Territories under U.S. Administration.

**Report of Investigations 9380**

# **Fire Detection for Conveyor Belt Entries**

**By Charles D. Litton, Charles P. Lauara,  
and Frank J. Perzak**

**UNITED STATES DEPARTMENT OF THE INTERIOR**  
**Manuel Lujan, Jr., Secretary**

**BUREAU OF MINES**  
**T S Ary, Director**

**Library of Congress Cataloging in Publication Data:**

**Litton, C. D. (Charles D.)**

Fire detection for conveyor belt entries / by Charles D. Litton, Charles P. Lazzara,  
and Frank J. Perzak.

p. cm. — (Report of investigations; 9380)

Includes bibliographical references (p. 14).

Supt. of Docs. no.: I 28.23:9380.

1. Coal mines and mining—Fires and fire prevention. 2. Fire detectors—Testing.  
3. Mine haulage—Safety appliances. I. Lazzara, Charles P. II. Perzak, F. J.  
(Frank J.) III. Title. IV. Series: Report of investigations (United States. Bureau  
of Mines); 9380.

TN23.U43 [TN315] 622 s—dc20 [622' .82] 91-23342 CIP

## CONTENTS

	<i>Page</i>
Abstract .....	1
Introduction .....	2
Description of experiments .....	3
Smoldering coal fires .....	5
Flaming coal fires .....	6
Growth rates .....	6
Carbon monoxide and smoke generation .....	7
Styrene-butadiene rubber belt fires .....	8
Polyvinylchloride belt fires .....	9
Fire detection .....	10
Sensor spacings and alarm thresholds .....	10
Nomograph usage—an example .....	12
Detector spacing—an example .....	13
Conclusions .....	13
References .....	14
Appendix A.—Heat-release rates .....	15
Appendix B.—Replacing point-type heat sensors .....	16
Appendix C.—Smoke optical density .....	19
Appendix D.—Effective entry <b>cross</b> section and <b>air</b> splits .....	20
Appendix E.—List of symbols .....	22

## ILLUSTRATIONS

1. Schematic of Lake Lynn aboveground fire gallery .....	4
2. Times to produce CO and smoke alarm levels for smoldering coal for an entry <b>cross</b> section of 7.53 m <sup>2</sup> .....	6
3. Production constant for CO for flaming coal fires .....	7
4. Production constant for smoke for flaming coal fires .....	8
5. Times to produce CO and smoke alarm levels for flaming coal fires for an entry cross section of 7.53 m <sup>2</sup> .....	8
6. Average times from belt ignition to onset of belt flame spread for SBR conveyor belts .....	9
7. Nomograph for CO sensor alarm thresholds and spacings .....	11
8. Nomograph for smoke sensor alarm thresholds and spacings .....	12
B-1. Thermal alarm times as function of <b>air</b> velocity for surface fire gallery tests .....	18
B-2. Thermal alarm times as function of entry cross section at velocities of 0.254 and 0.508 m/s .....	18

## TABLES

1. Description of conveyor belt tested .....	4
2. Measured and predicted CO levels for smoldering coal dust just <b>prior to flaming</b> .....	5
3. Estimated optical density levels at time of smoke alarm .....	5
4. Large-scale gallery test data for ignition of rubber belts .....	7
5. Large-scale gallery test data for SBR belt fires .....	9
6. Times to belt ignition and peak fire intensities for PVC conveyor belt .....	10
7. <b>Location</b> of sensors along example belt entry .....	13
A-1. Values of H <sub>c</sub> , X <sub>c</sub> , k <sub>CO<sub>2</sub></sub> , and k <sub>CO</sub> for combustibles used in experiments .....	15

## UNIT OF MEASURE ABBREVIATIONS USED IN THIS REPORT

<b>°C</b>	degree Celsius	<b>kW</b>	<b>kilowatt</b>
<b>cm</b>	centimeter	<b>kW/min</b>	kilowatt per minute
<b>°F</b>	degree Fahrenheit	<b>m</b>	meter
<b>ft</b>	foot	<b>m<sup>-1</sup></b>	inverse meter
<b>ft<sup>2</sup></b>	square foot	<b>m<sup>2</sup></b>	square meter
<b>ft/min</b>	foot per minute	<b>m<sup>3</sup></b>	cubic meter
<b>g</b>	gram	<b>min</b>	minute
<b>g/g</b>	<b>gram per gram</b>	<b>mm</b>	millimeter
<b>g/m<sup>3</sup></b>	gram per cubic meter	<b>μm</b>	micrometer
<b>g/s</b>	gram per second	<b>m<sup>3</sup>/min</b>	cubic meter per minute
<b>kg</b>	<b>kilogram</b>	<b>m/s</b>	meter per second
<b>kg/m</b>	kilogram per meter (linear)	<b>ppm</b>	part per million
<b>kJ</b>	kilojoule	<b>s</b>	second
<b>kJ/g</b>	kilojoule per gram	<b>V</b>	volt
<b>kJ/m</b>	kilojoule per meter	<b>W</b>	watt

# FIRE DETECTION FOR CONVEYOR BELT ENTRIES

By Charles D. Lion,<sup>1</sup> Charles P. Lazzara,<sup>2</sup> and Frank J. Perzak<sup>3</sup>

---

## ABSTRACT

**This** U.S. Bureau of Mines report details the results of a series of large-scale experiments where small coal fires were used to ignite the conveyor belt at **air** velocities ranging from 0.76 to 6.1 m/s. In the tests, electrical strip heaters imbedded within a pile of coal were used to heat the coal to a point of flaming ignition. The flaming coal subsequently ignited the conveyor belt located approximately 5 to 10 cm above the coal pile. During the tests, temperature, CO, and smoke levels were continuously measured in order to determine both alarm time and level **as** the fire intensity progressed through the stages of smoldering **coal**, flaming **coal**, and flaming coal plus *flaming* belt.

Analysis of the data leads to certain conditions of **air** velocity and sensor alarm levels that **are** required for early detection of conveyor belt entry fires. Two nomographs are presented, which define sensor alarm levels and sensor spacings **as** a function of belt entry cross-sectional area and belt entry **air** velocity.

---

<sup>1</sup>Supervisory physical scientist.

<sup>2</sup>Supervisory research chemist.

<sup>3</sup>Research chemist.

Pittsburgh Research Center, U.S. Bureau of Mines, Pittsburgh, PA.

## INTRODUCTION

Fire represents one of the most severe hazards in underground coal mines. The heat and combustion products liberated are carried downstream from the fire by the ventilation airflow, eventually contaminating areas of a mine far removed from the fire. The ventilation airflow serves to dilute the combustion products, thus lowering their concentration. The higher the airflow, the greater the dilution. Combustion products also spread more rapidly at higher air velocities than at lower air velocities. These effects are somewhat obvious. The effects that the airflow has on the growth and burning characteristics of the fire are not so obvious.

For many fires that develop within conveyor belt entries, it is found that coal heats to the point of flaming because of frictional overheating in the belt drive area or near idlers along the belt structure. When the conveyor belt is stopped, the coal fire then spreads to the conveyor belting, and if the conveyor belt has poor flame-resistant properties, the flame will begin to propagate along the exposed surfaces of the conveyor belt. As the surface area of the burning conveyor belt increases, so does the total fire intensity, along with increases in the levels of smoke and CO that are produced. Typical fires in belt entries develop in three *distinct* stages:

1. Early smoldering stages of coal heated, due to overheated equipment or friction, to the point of flaming;
2. Early flaming stages of a small coal fire, which ignites a stationary conveyor belt;
3. Combined coal and conveyor belt fire, which increases in intensity to the point of sustained belt flame spread.

The time it takes for the fire to develop through these various stages depends upon many factors. The duration of the smoldering stage depends upon the temperatures of the overheated equipment, the quantity of coal involved, and the proximity of the source of heating to the exposed surfaces of the coal pile. The size of the coal (i.e., dust or lumps, or a mixture of the two) also has an effect. **This** stage of development may take minutes or hours before the coal begins to flame. During **this** stage, CO and smoke are produced, with the quantities produced depending upon the size of the coal, the mass of the coal, the temperature of the coal mass involved, and other factors.

Once ignited, the coal fire intensity begins to increase. The rate of increase depends upon the **air** velocity and the surface area of coal available for burning. Subsequent ignition of the conveyor belt depends upon the proximity of the belt to the coal fire, the thermal characteristics of

the belt material, and the air velocity. Once the belt ignites, usually near the lateral edges of the belt, the flame **will** begin to spread over the surface of the belt in the vicinity of the source coal fire. The rate of spread, locally, depends upon the air velocity and the flame-spread characteristics of the belt material. If the belt material has poor flame-resistant properties (i.e., it propagates flame easily), the combined local coal and belt fire **will** attain sufficient intensity so that the flame begins to spread away from the original ignition area along the exposed surfaces of the belt and in the direction of the airflow. If the belt has good flame-resistant properties (i.e., it is difficult to propagate flame), local burning will occur only in the vicinity of the coal fire, with **no** propagation of the flame along the belt surfaces. For a conveyor belt with poor flame-resistant properties, the time it takes for the fire to begin to propagate downstream, away from the ignition area, depends upon the air velocity and the flame-spread characteristics of the belt material.

In general, if the fire reaches a *size* sufficient to begin flame spread down the belt, the effectiveness of control and extinguishment procedures *diminishes* rapidly. In addition, the levels of smoke and CO produced begin to approach dangerous levels, and lethal levels may subsequently result during the propagation stage. Consequently, for fires in belt entries, all evacuation and control procedures should be implemented prior to the onset of belt flame spread.

Clearly, any measure that **can** be taken to reduce or eliminate the possibility of the occurrence of belt fires should be done. For instance, diligent housekeeping procedures to eliminate coal spillage in a belt drive-belt takeup area reduces the potential for the source coal fire to develop. Maintaining slippage switches to reduce the occurrence of frictional heating also reduces the potential for development of the fire. Along the belt entry, continuous vigilance for overheated idlers, which **can** serve as the initiator for the fire, is beneficial. Use of belt materials that have superior fire-resistance characteristics will reduce the possibility of belt flame spread (1).<sup>4</sup> Automated extinguishment systems that are activated in the early stages of fire development **can** reduce the potential for belt flame spread.

The occurrence of any fire at any stage of development represents a potential hazard to underground personnel. If, and when, a fire develops, the detection of that fire at the earliest possible moment is paramount to secure the

---

<sup>4</sup>Italic numbers in parentheses refer to items in the list of references preceding the appendixes at the end of this report.



safety of underground personnel and **successfully** control and extinguish the fire. It is obvious that detection of any developing fire prior to open **flaming** is always desirable. If the duration of **this** stage of development is long (several minutes to an hour, or longer) and a sufficient mass of **coal** (or other combustible) is involved, the probability of detecting the fire during **this** stage **will** be high. However, a small flaming coal fire may result from an intense smoldering stage that may last only a few minutes and may initially involve a small mass of coal. For this situation, the probability of detecting the fire in its smoldering stage is reduced.

In general, a flaming coal fire follows the smoldering stage of development. During **this** flaming stage, the fire may grow in intensity **until**, eventually, the conveyor belting

is ignited. The probability of detecting a fire in **this** stage of development depends upon how fast the fire grows and at what fire **size** belt ignition is achieved. The slower the growth rate of the flaming coal fire, the higher the probability that it **can** be detected prior to belt ignition.

It is imperative that the relative times for transition of the fire from one stage to the next, along with the levels of CO and smoke produced during each stage, be quantified **as** accurately **as** possible. To obtain **this** information, the **U.S.** Bureau of Mines conducted a series of large-scale gallery tests at **air** velocities from 0.76 up to 6.1 m/s using a small coal fire to ignite rubber and polyvinyl chloride (PVC) belt materials. This work was done **as** part of the Bureau's program to enhance mine safety.

## DESCRIPTION OF EXPERIMENTS

The large-scale experiments for belt fire detection were conducted in the Bureau's aboveground fire gallery located at Lake **Lynn** Laboratory. The fire gallery **consists** of a 27.4-m-long tunnel constructed of masonry block walls, a steel arched roof, and a concrete floor. The tunnel is coupled to a 1.8-m-diameter, **3,500-m<sup>3</sup>/min** axivane fan via a 6-m-long tapered transition section. The ventilation flow **can** be varied by adjusting the pitch of the fan blades and/or by throttling the fan intake. **A** schematic of the gallery is shown in figure 1. The cross-sectional area of the tunnel is **7.53 m<sup>2</sup>**. The interior walls and roof of the tunnel are covered with ceramic blanket insulation. Tunnel distances are measured from the junction of the fire tunnel and transition section, designated **as** the 0m mark. A typical conveyor belt frame, 21 m long and 1.5 m wide, is centered in the tunnel. The frame **consists** of a 0.4-m-diameter tail pulley and 0.7-m-diameter troughed idler assemblies spaced at 1.2-m intervals.

A small coal pile fire, located just downstream of the tail pulley, was the ignition source for the tests. The 0.5-m-deep coalbed, supported **on** a steel grate, consisted of about 320 kg of **5 cm** or smaller pieces of Sewickley seam coal (**35%** volatile matter, 14% ash), with a minimum of fines. The top surface of the pile was 0.6 m long (along the length of the belt structure) by 0.9 m wide. To initiate a coal fire, **six** electrical strip heaters (three from each side) were imbedded about **5 cm** below the top surface of the pile. Each strip heater was 1.9 cm wide by **49 cm** long (heated length of **40 cm**) and was rated at 1,000 W at 240 V. The voltage to the strip heaters was controlled by a variable transformer. For a test, the heater voltages were maintained **as** follows: **0 to 5 min**, 80 V; **5 to 15 min**, 140 V; and 15 min to shut off, 190 V. The

heaters were turned **off** after the coal fire ignited the belt sample and the belt fire **was** well developed in the **ignition** area.

Typically, a 6.2-m-long sample of conveyor belting, with the top cover up if applicable, **was** placed **on** the rollers of the belt structure, stretched over the coal pile, and fastened to the **tail** pulley. The distance from the top surface of the coal pile to the bottom surface of the belt sample was **5 to 10 cm**, and the distance of the belt sample to the tunnel roof was about 1.2 m. Thermocouples were imbedded just below the top surface of the belting, starting at a point above the coal pile and continuing 4.6 m downstream, to determine when the fire spread out of the ignition area.

The gallery was instrumented with thermocouples to measure gas temperatures. **An** array of **12** thermocouples, connected in parallel and distributed over the **cross-sectional** area of the tunnel, **was** located at 24.4 m to measure the average temperature of the stratified **gas** exit stream.

**A** gas and smoke sample averaging probe was positioned at a tunnel distance of 25.9 m, about 21.4 m downstream of the coal pile fire. **This** probe, constructed from nominal **5-cm-diameter** steel pipe, had four inlet ports spaced along the vertical height of the tunnel in order to estimate the average smoke and gas concentrations in the exit gas stream. The sample was analyzed for smoke, CO, and CO<sub>2</sub>. **In** addition, a smoke and a CO **fire** detector were located near the roof of the tunnel near **the** exit at the 26.7-m tunnel position.

The outputs of the thermocouples and analyzers were connected **to** a 60-channel microprocessor that **transmits** the data to a computer for storage. The data were **logged**

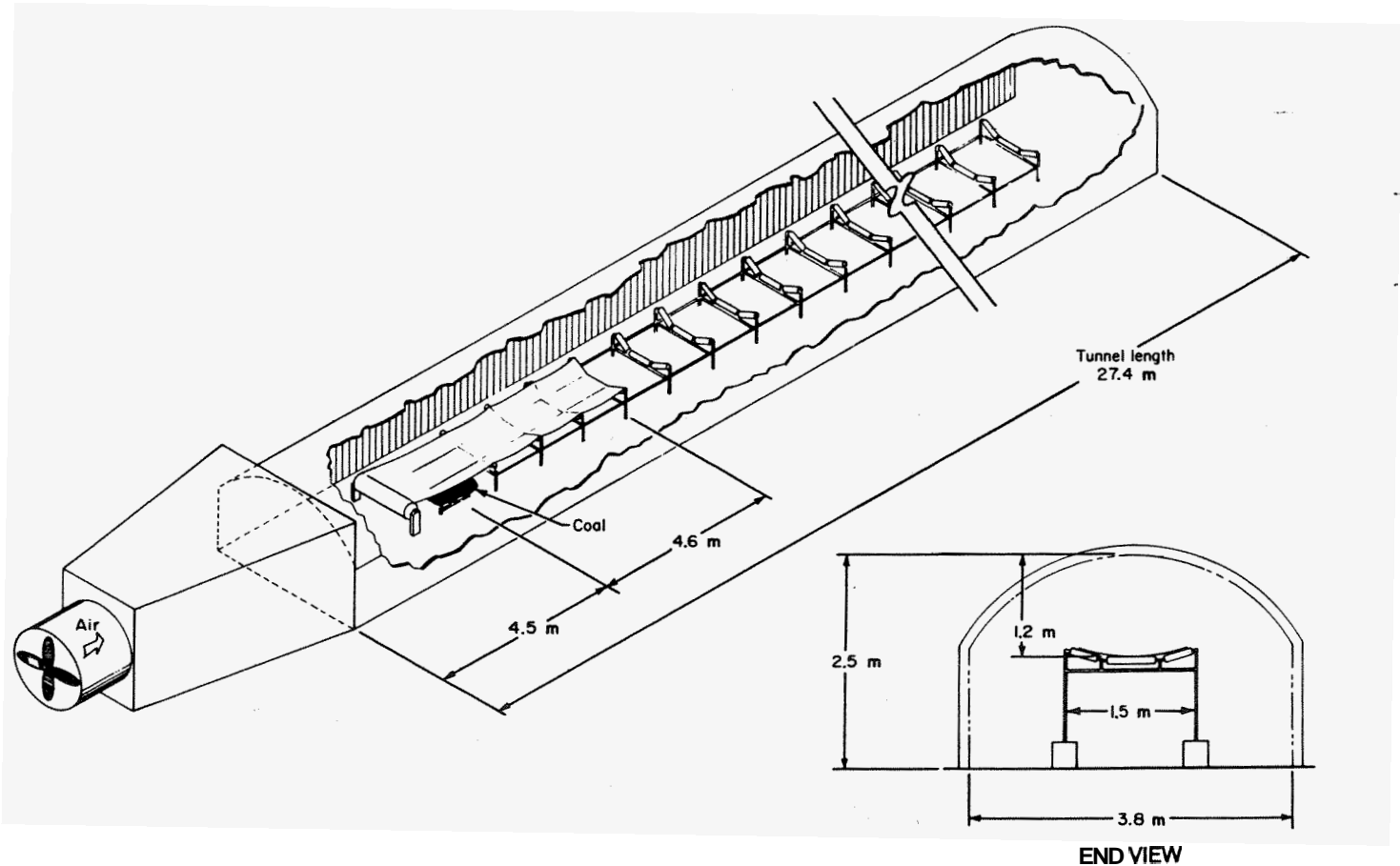


Figure 1.—Schematic of Lake Lynn aboveground fire gallery.

at 15-s intervals and displayed on a computer terminal. After a test, time-temperature traces and gas concentration plots were generated from the stored data. The experiments were also recorded on videotape.

The experiments were conducted at gallery airflows of 0.76, 1.52, 4.06, and 6.1 m/s. The airflow was measured prior to the start of a test by a handheld anemometer across the width of the belt sample (at a height of 25 cm above the belt) and at three locations along the sample length, and then these values were averaged. The average airflow near the exit of the tunnel was also measured. The airflow fluctuated, especially at the high flows, but was within  $\pm 15\%$  of the selected value.

A description of the conveyor belting tested is given in table 1. All the belts were obtained new from cooperating belt manufacturers. Belt R1 is considered to be non-fire-resistant because it failed the current small-scale Federal approval test for fire-resistant belting (2). Belts R4, R11, and P1 passed the test and were considered fire-resistant. Belts R11 and P1 were tested at all four airflows, while belt R4 was tested only at 1.52 m/s. and belt R1 at airflows of 0.76, 1.52, and 4.06 m/s.

Table 1.—Description of conveyor belt tested

Belt	Construction	Width, m	Thickness, mm	Weight, kg/m	Fire-resistant quality
R1 ...	4-ply SBR, 7-mm top cover, 2-mm bottom cover.	1.07	15	17.8	NFR
R4 ...	Chloroprene, solid woven, 3-mm top cover, 2-mm bottom cover.	1.07	9	14.3	FR
R11 ..	3-ply SBR, 5-mm top cover, 2-mm bottom cover.	1.07	11	14.9	FR
P1 ...	Solid woven PVC	1.07	11	14.2	FR
FR	Fire-resistant. Passed Federal approval test (2).				
NFR	Non-fire-resistant. Failed Federal approval test (2).				
PVC	Polyvinyl chloride.				
SBR	Styrene butadiene rubber.				

## SMOLDERING COAL FIRES

In the experiments, the period of smoldering of the coalbed prior to flaming is controlled primarily by the time required to raise the surface temperature of the strip heaters to temperatures sufficient to ignite the coal. For all tests conducted, the average time from the start of the test until the time that flames were first observed on the coal pile was  $23.1 \pm 3.0$  min. On the average, the time of smoldering (as measured from the time of first visible smoke until the time of flaming) was 10 min. It is during this period that low levels of smoke and CO are produced, and even though the duration of this period is controlled by the heater temperature, the levels of CO produced just prior to flaming can provide some insight as to the influence of air velocity on the generation rates of CO in these experiments.

At any point in time, the levels of CO produced within an entry with a defined airflow rate can be expressed as

$$\text{ppm CO} = \frac{\dot{G}_{\text{CO}}}{v_o A_o}, \quad (1)$$

where  $\dot{G}_{\text{CO}}$  = generation rate of CO,  $\frac{\text{ppm} \cdot \text{m}^3}{\text{s}}$ ,

$v_o$  = air velocity, m/s,

and  $A_o$  = entry cross-sectional area,  $\text{m}^2$ .

In a dynamic situation,  $\dot{G}_{\text{CO}}$  is not constant, but increases with time.  $\dot{G}_{\text{CO}}$  may also depend upon  $v_o$ . To determine if  $\dot{G}_{\text{CO}}$  is air velocity dependent, the average levels of CO existing just prior to flaming were measured and  $\dot{G}_{\text{CO}}$  was determined from equation 1. Also, the change in  $\dot{G}_{\text{CO}}$ ,  $\Delta \dot{G}_{\text{CO}}$ , measured during the smoldering interval,  $\Delta t$ , was put in the form

$$\frac{\Delta \dot{G}_{\text{CO}}}{\Delta t} = \alpha, \quad (2)$$

where  $\alpha$  = average rate of production of CO during  $\Delta t$ .

The value of  $\alpha$  was tabulated for all tests and then the average value at each air velocity was determined. A least-squares regression of the data yielded the expression

$$\alpha = 2.4 + 1.6 v_o. \quad (3)$$

Equation 1 can then be written as

$$\text{ppm CO} = \frac{(2.4 + 1.6 v_o)}{v_o A_o} \cdot t, \quad (4)$$

where the time,  $t$ , is measured from the onset of smoldering.

Using equation 4, the measured and predicted levels of CO, just prior to flaming, are compared in table 2.

Table 2.—Measured and predicted CO levels for smoldering coal dust just prior to flaming

$v_o$ , m/s	$t_s$ , min	CO, ppm	
		Measured	Predicted
0.76	11.8	6.7	7.4
1.52	11.2	4.6	4.7
4.06	8.7	3.3	2.5
6.1	6.2	1.3	1.6

Equation 4 can also be used to predict the time,  $(t_A)_{\text{CO}}$ , a smoldering period would have to exist until certain levels of CO are formed that are equal to the CO sensor alarm thresholds,  $\text{CO}_A$ , in parts per million. The equation that defines this time is given by

$$(t_A)_{\text{CO}} = \frac{\text{CO}_A \cdot v_o A_o}{\alpha} \quad (5)$$

For smoke sensors, previous data (3) from tests in an intermediate-scale fire tunnel indicate that the average rate of smoke production,  $G_s$ , where the subscript "D" refers to optical density of the smoke (see appendix C), from smoldering coal fires is 0.024 times the rate of CO production. By using one-half this value for an increased safety factor, the time,  $(t_A)_D$ , for the smoldering coal fire to produce some specified smoke alarm threshold level,  $D_A$ , (units of inverse meters) is given by the expression

$$(t_A)_D = \frac{D_A v_o A_o}{0.012 \cdot \alpha}. \quad (6)$$

In the large-scale gallery tests, the average times of actual smoke detector alarm, as measured from the time of first visible smoke, can be used in equation 6 to determine the approximate levels of optical density existing at the time of alarm. These levels are computed in table 3.

Table 3.—Estimated optical density levels at time of smoke alarm

Air velocity, m/s	Average time to smoke sensor alarm, min	Estimated optical density, $\text{m}^{-1}$
0.76	8.3	0.063
1.52	7.0	.035
4.06	9.2	.032

For the two tests conducted at an air velocity of 6.1 m/s, coal flame occurred at 8.4 min in the first test and at 4.0 min in the second test. For these two tests, the estimated smoke optical densities just prior to flaming are 0.026 m<sup>-1</sup> and 0.013 m<sup>-1</sup>, respectively. Based upon the estimated alarm values from table 3, the levels of 0.026 and 0.013 m<sup>-1</sup> were below the alarm threshold level for the smoke sensor. At this velocity, a smoldering period of about 14.0 min would have been sufficient to produce alarm prior to the onset of flaming, as shown in figure 2.

Figure 2 is a plot of the approximate smoldering times necessary to produce the indicated CO and smoke alarm levels as a function of the air velocity. Figure 2 also shows the average smoldering times,  $t_s$ , observed in the experiments at each air velocity. These data indicate that at higher air velocities, the duration of the smoldering period decreases. When the velocity exceeds about 2.54 m/s, the smoldering stage would not be detected by either 5 ppm CO sensors or 0.044 m<sup>-1</sup> smoke sensors.

The generation rates of CO and smoke discussed above are specific to the arrangement of the experiment. For example, if more heaters were used, the coal surface area subjected to heating would increase, thus increasing the rates of production of CO and smoke. The surface area of a typical bottom roller along a conveyor belt is about 0.5 m<sup>2</sup> compared with the total surface area of the strip heaters used in the experiments of about 0.10 m<sup>2</sup>. Thus, if the surface temperature of the roller reached 500° C, typical of the heater surface temperature of the strip heaters, about five times more CO and smoke would be produced than experimentally observed. Fewer heaters (less surface) would have produced less CO and smoke. If the surface temperature of the heaters was lower than that used in the experiments, less CO and less smoke would be produced. The experimental arrangement was

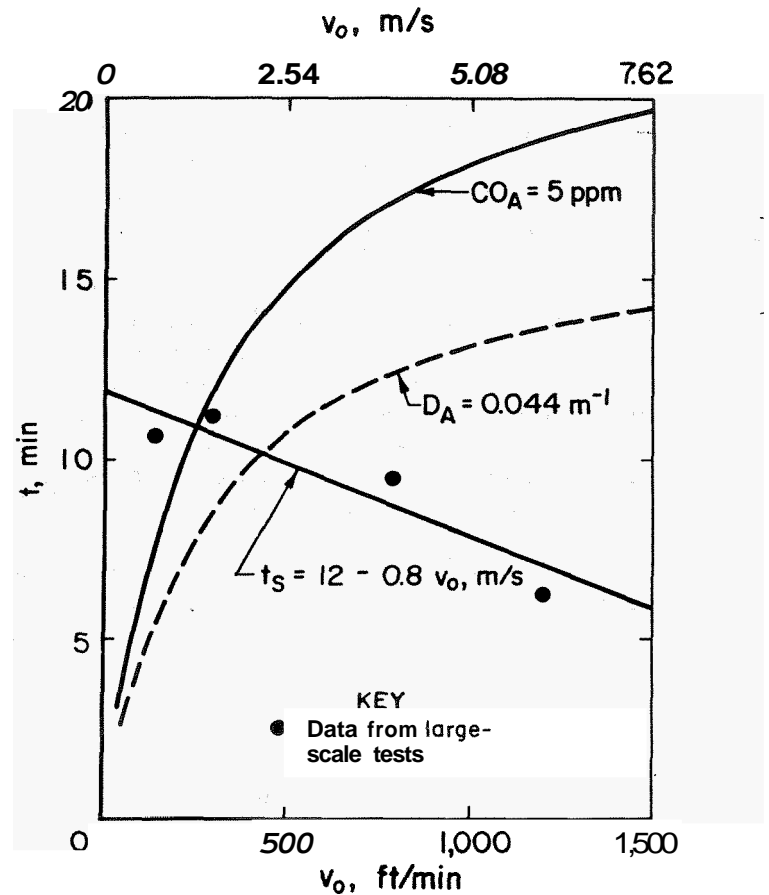


Figure 2.—Times to produce CO and smoke alarm levels for smoldering coal for an entry cross section of 7.53 m<sup>2</sup>.

intentionally sized to create a small coal fire sufficient to ignite the belt within a reasonable time.

## FLAMING COAL FIRES

### GROWTH RATES

In the large-scale gallery tests, the times from the instant of flaming ignition of the coalbed until the instant that flames were first observed on the conveyor belt were measured. The fire intensity at the moment of belt ignition was then calculated from the CO<sub>2</sub> and CO gas levels as outlined in appendix A. At the time of belt ignition, the coal fires were still quite small, so there exists some degree of uncertainty in the measured gas levels.

The total heat-release rates from the coal fire,  $\dot{Q}_{\text{COAL}}$ , at the time of belt ignition; the time elapsed from the moment of coal ignition until the moment of belt ignition,  $t_{\text{BI}}$ ; the rate of increase of the fire intensity during this time,  $\alpha_{\text{COAL}}$ ; and the ratio of fire intensity to ventilation

velocity,  $\dot{Q}_{\text{COAL}}/v_0$ , at the time of belt ignition for tests conducted with rubber conveyor belting at indicated  $v_0$  are shown in table 4.

Using the average values of  $\alpha_{\text{COAL}}$  at each air velocity, a least-squares regression of the data yields the expression

$$\alpha_{\text{COAL}} = 1.65 + 0.90 v_0. \quad (7)$$

The rate of increase of the coal fire intensity is then given by the expression

$$\dot{Q}_{\text{COAL}} = \alpha_{\text{COAL}} \cdot t, \quad (8)$$

where  $t$  is measured from the time of first observed coal flames.

Table 4.—Large-scale gallery test data for ignition of rubber belts

Belt	Test	$v_o$ , m/s	$Q_{COAL}$ , kW	$t_{BI}$ , min	$\alpha_{COAL}$ , kW/min	$Q_{COAL}/v_o$ , kJ/m
R11 ..	81A	0.76	20	8.5	24	26.3
R1 ...	82	.76	25	13.0	1.9	33.1
R11 ..	78	1.52	60	26.0	2.3	39.1
R4 ...	79	1.52	50	12.0	4.2	33.1
R1 ...	84	1.52	40	11.0	3.6	16.6
R11 ..	85	1.52	30	6.0	5.0	19.6
R1 ...	77	4.06	140	24.5	5.7	34.6
R11 ..	80	4.06	95	20.0	4.8	23.3
R11 ..	83	6.10	NA	24.6	NA	NA
NA	Not available.					

From column 7 of table 4, it is also found that the average ratio of fire intensity to ventilation velocity is 28.2 at the time of belt ignition for the rubber conveyor belts. This means that the fire intensity sufficient to ignite the belt is a linear function of air velocity.

### CARBON MONOXIDE AND SMOKE GENERATION

For open, flaming fires, the generation rates of CO and smoke are dependent upon the total heat-release rates via the expressions

$$\dot{G}_{CO} = B_{CO} \cdot \dot{Q}_{COAL}, \quad (9)$$

and 
$$\dot{G}_D = B_D \cdot \dot{Q}_{COAL}, \quad (10)$$

where  $B_{CO}$  and  $B_D$  = production parameters for CO and smoke, respectively.

Because this stage of fire development is that of open, flaming combustion, the rates of production of CO and smoke depend upon the stoichiometry of the fuel-air mixture that is reacting. As the fuel-air mixture decreases from its stoichiometric level toward its lean limit of flammability, the levels of CO and smoke produced will also decrease. At the other extreme, as the fuel-air mixture increases above its stoichiometric level toward its rich flammability limit, the levels of CO and smoke produced will increase.

In the early stages of fire growth, excess air is usually available for combustion of the fuel. As a result, such fires will generally burn on the lean side of the stoichiometric level. Further, the rates of production of CO and smoke are sensitive to the fuel-air mixture on the lean side, and it is these rates of production that determine the ability of CO and smoke fire sensors to detect fires in their early stages of flaming.

To determine what, if any, effect air velocity has on the production of CO and smoke, the data were analyzed as a function of the air velocity. These data were supplemented by a series of tests of small coal fires in an intermediate-scale fire tunnel at air velocities ranging

from 0.53 to 7.7 m/s. During the intermediate-scale fire tests, the optical density of the smoke was also measured.

Figure 3 is a plot of the combined data for CO from both the large-scale gallery and the intermediate-scale tunnel tests showing that the coal fires produced less CO at the higher air velocities. As a result of this behavior, the times to reach an alarm level of CO, during the growth stages of a coal fire, depend not only upon the growth rate of the fire, but also upon the rates of production of CO, both quantities being dependent upon the ventilation air velocity.

Data for the smoke optical density acquired in the supplemental intermediate-scale tests are shown in figure 4. For smoke, the production rate shows a similar dependence on air velocity as observed for CO. Previous data for smoke production from coal fires were obtained at an air velocity of 0.38 m/s and yielded a value of 0.036 for  $B_D$ , which agrees with the data of figure 4 (4).

As was the case for the smoldering coal fires, equations 7 through 10 may be used to estimate the times for small flaming coal fires to generate alarm levels of CO and smoke. For CO, the expression is

$$(t_A)_{CO} = \frac{CO_A \cdot v_o A_o}{B_{CO} \cdot \alpha_{COAL}}, \quad (11)$$

while for the smoke, the expression is

$$(t_A)_D = \frac{D_A \cdot v_o A_o}{B_D \cdot \alpha_{COAL}}. \quad (12)$$

The resulting curves are shown in figure 5, where the time is measured from the instant of flaming ignition, assuming no smoldering exists prior to flaming. The results of this analysis are similar to those for the smoldering case. Figure 5 also shows the average times, denoted by  $t_f$ , at each air velocity, between coal ignition and belt ignition.

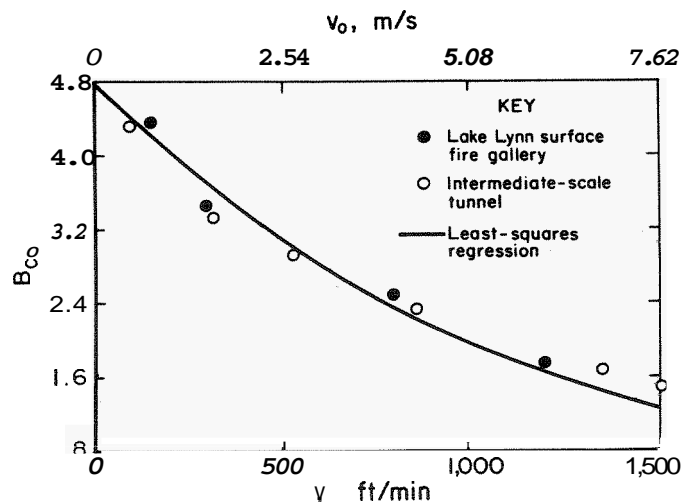


Figure 3.—Production constant for CO for flaming coal fires. The curve is defined by the expression  $B_{CO} = 4.80 e^{-0.175 v_o \text{ m/s}}$ .

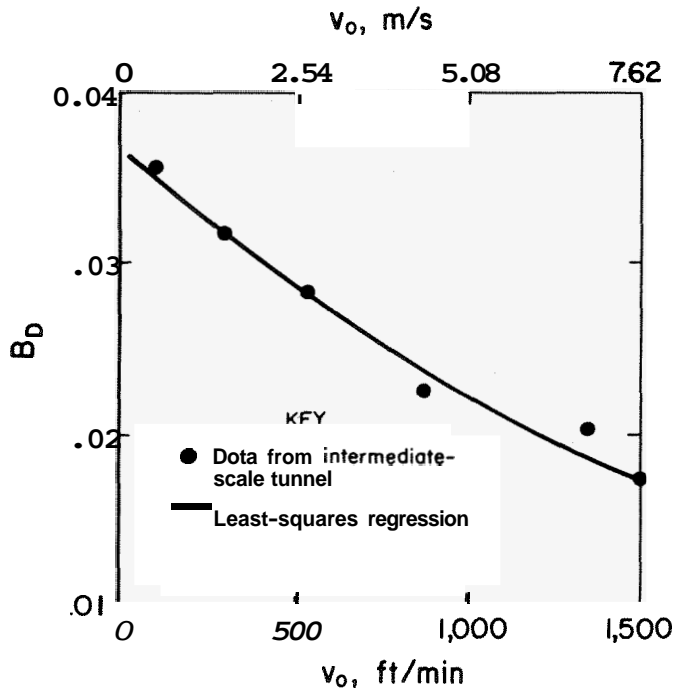


Figure 4.—Production constant for smoke for flaming coal fires. The curve is defined by the expression  $B_D = 0.037 e^{-0.1v_o, \text{ m/s}}$ .

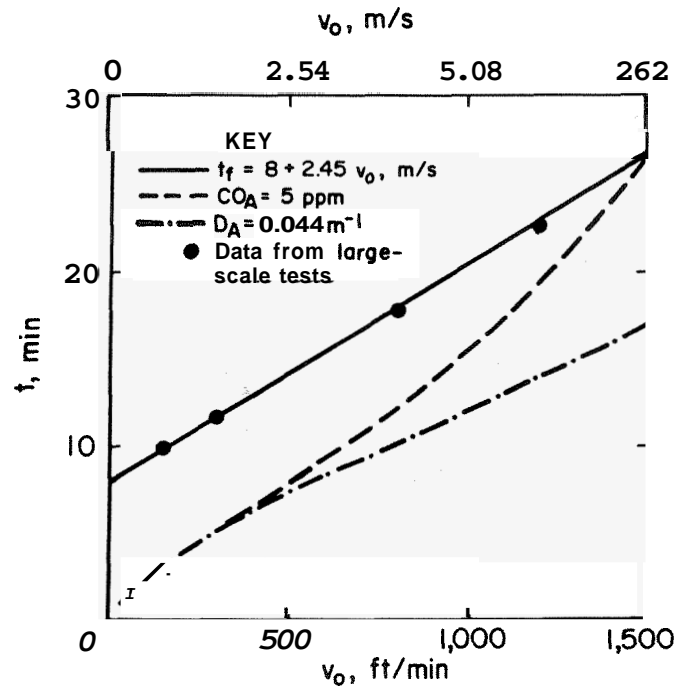


Figure 5.—Times to produce CO and smoke alarm levels for flaming coal fires for an entry cross section of  $7.53 \text{ m}^2$ .

## STYRENE-BUTADIENE RUBBER BELT FIRES

Once the small coal fire ignites the belt, the total heat-release rate increases dramatically because of the additional fuel supplied by the belt. The total fire intensity during this stage of fire development is due to both the coal fire and the styrene-butadiene rubber (SBR) belt fire. To determine the rate of growth of the belt fire and the ratio of total fire intensity to ventilation airflow at the beginning of belt flame spread,  $t_{\text{BFS}}$ , the total fire intensity,  $Q_{\text{TOTAL}}$ , was determined at the time the belt flame spread began. The coal fire intensity at this time was determined from equation 8 and subtracted from the total fire intensity. This fire intensity difference was then assumed to be due **only** to the burning belt, and when this quantity is divided by the difference in time between  $t_{\text{BFS}}$  and  $t_{\text{BI}}$ , the growth rate of the conveyor belt portion of the fire can be determined. The data used to make these determinations are shown in table 5.

From the data in table 5, it is found that the average ratio of total fire intensity to ventilation velocity was 323, independent of the air velocity, at  $t_{\text{BFS}}$ . It was also determined that the fire growth rate for the belt could best be put in the form

$$\dot{Q}_{\text{SBR}} = \alpha_{\text{SBR}} \cdot (t - t_{\text{BI}}), \quad (13)$$

where  $\dot{Q}_{\text{SBR}}$  = heat-release rate of SBR conveyor belt fire, kW,

and  $\alpha_{\text{SBR}}$  = growth-rate parameter for SBR conveyor belt fire, kW/min.

A least-squares regression analysis of the average values of  $\alpha_{\text{SBR}}$  obtained at each air velocity yielded the expression

$$\alpha_{\text{SBR}} = (14.0 + 1.5 v_o) v_o, \quad (14)$$

The average times at each air velocity between belt ignition and belt flame spread are shown in figure 6. As the air velocity increases, this time gradually decreases. For the fire-resistant rubber belting (R11), the rates of generation of CO were found to be constant with a  $B_{\text{CO}}$  value of 5.68, independent of the air velocity. Using previous data (3) for smoke levels, the  $B_{\text{D}}$  value for these belts is 0.062.

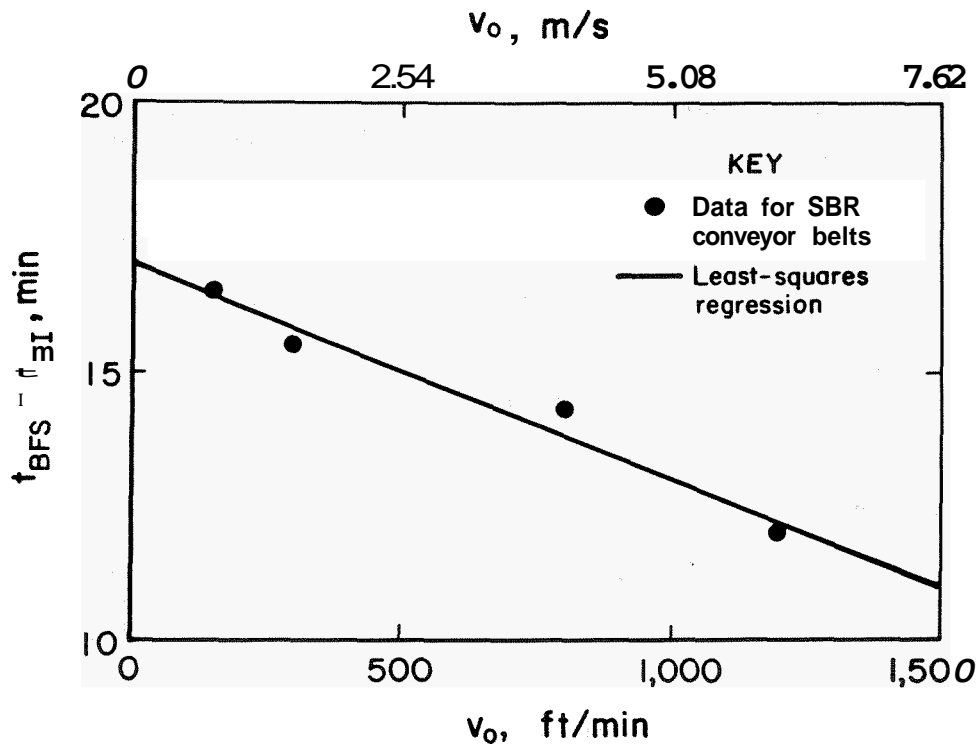


Figure 6.—Average timer from belt ignition to onset of belt flame spread for SBR conveyor belts. The curve is defined by the expression  $t_{BFS} - t_{BI} = 17 - 0.8v_o$ , m/s.

Table 5.—Large-scale gallery test data for SBR belt fires

Belt	Test	$v_o$ , m/s	$Q_{TOTAL}$ , kW	$t_{BFS}$ , min	$Q_{COAL}$ , kW	$Q_{SBR}$ , kW	$t_{BFS} - t_{BI}$ , min	$\alpha_{SBR}$ , kW/min	$Q_{TOTAL}/v_o$ , kJ/m
R11 ..	81A	0.76	250	24.0	61	189	15.5	12.2	328
R1 ...	82	.76	245	30.5	78	167	17.5	9.5	321
R11 ..	78	1.52	480	44.5	142	338	18.5	18.3	315
R1 ...	84	1.52	515	23.0	73	442	11.0	38.1	338
R11 ..	85	1.52	490	23.0	73	417	17.0	24.5	321
R1 ...	77	4.06	1,270	37.5	201	1,069	13.0	82.2	312
R11 ..	80	4.06	1,320	35.5	190	1,130	15.5	72.9	325
R11 ..	83	6.1	1,970	36.5	259	1,711	12.0	142.6	323

## POLYVINYL CHLORIDE BELT FIRES

For tests conducted with PVC conveyor belting, it was found that the P1 belt was more readily ignitable by the small coal fires than the SBR belt. However, it was also found that the P1 belt did not propagate flame. The data for this series of tests with the P1 belt are shown in table 6. At ignition of the P1 belt, the ratio of coal fire intensity to ventilation velocity was dependent upon the air velocity according to the expression

$$Q_{COAL}/v_o \geq 27.5e^{-0.13v_o} \quad (15)$$

It was also found that once the P1 conveyor belt ignited, its rate of fire growth was less than that for

the SBR belt. For the PVC belt, the fire growth rate parameter was found to be

$$\alpha_{PVC} = (7.0 + 0.95 v_o) v_o^{1/2}, \quad (16)$$

where  $\alpha_{PVC}$  = growth-rate parameter for PVC conveyor belt fire, kW/min,

with the resultant fire growth rate given by

$$\dot{Q}_{PVC} = \alpha_{PVC} \cdot (t - t_{BI}), \quad (17)$$

where  $\dot{Q}_{PVC}$  = heat-release rate of PVC conveyor belt fire, kW.

**Table 6.—Times to belt ignition and peak fire intensities for PVC conveyor belt**

Test	$v$ m/s	$t_{BI}$ min	$\dot{Q}_{COAL}$ kW	$\dot{Q}_{COAL}/v_o$ kJ/m	$t_{PEAK}$ min	$\dot{Q}_{PVC}$ kW	$\alpha_{PVC}$ kW/min
86 ...	1.52	6.6	39.0	25.7	15.1	130	15.3
101 ..	1.52	6.0	27.0	17.8	25.9	118	5.9
102 ..	4.06	10.7	34.0	8.4	<b>20.0</b>	233	25.1
105 ...	.76	6.6	20.0	26.3	17.5	80	7.3
106 ..	6.10	18.0	80.0	13.1	24.5	217	33.4
107 ..	4.06	<b>20.8</b>	92.0	22.7	<b>28.3</b>	<b>127</b>	16.9

## FIRE DETECTION

When a fire occurs, three events must take place in order for the fire to be detected.

1. The fire must be large enough to produce alarm levels of the fire characteristic that is to be detected. For instance, if the fire characteristic to be detected is CO and the alarm level is 5 ppm of CO, then the fire must be large enough to produce 5 ppm of CO within the ventilation airflow. This implies, then, that a finite amount of time must elapse before this event *can* occur. The estimated times for specified alarm levels of CO and smoke, based upon the data obtained in the experiments, are shown in figures 2 and 5. Lower alarm levels *will* require less time for this event to occur, while higher alarm levels will require more time.

2. Once a characteristic alarm level has been reached at the fire source, then this level of CO or smoke must be transported from the fire to the sensor location by the ventilation airflow. For fires along conveyor belt entries, the **maximum** transport time is equal to the sensor spacing divided by the ventilation **air** velocity. For instance, if the sensor spacing is 304.8 m (1,000 ft) and the air velocity is 1.016 m/s (200 ft/min), then the **maximum** transport time is 300 s (5 min). In general, the location of fires along conveyor belt entries is most uncertain. As a consequence, the probability that a fire will occur very close to a sensor is the same as for a fire occurring one sensor spacing from the sensor. On the average, then, CO or smoke *will* have to be transported a distance equal to one-half the sensor spacing,  $\ell_s$ . The transport time,  $t_t$ , in minutes, then, *can* be defined by

$$t_t = \frac{1}{2} \left[ \frac{\ell_s}{60 v_o} \right]. \quad (18)$$

The belt drive area will be protected by sensors at maximum distances of about 30.5 m from the belt drive area. For these cases, the transport time is relatively short owing to the small distance involved.

For the P1 belt, the CO data yielded an average value of  $B_{CO} = 11.2$ , a factor of 2 greater than that for the rubber belts. Again, using previous data (3) for the relative smoke level, the  $B_D$  value for the P1 belt is 0.072.

For both the PVC and SBR belts, the time from belt ignition necessary to produce CO and smoke alarm levels is very short because of the large growth rates of the belt fires. Burning belts typically produce sufficient CO and smoke to meet or exceed sensor alarm levels within several seconds from the time that they are ignited.

3. Once the above level of CO or smoke reaches the sensor, then the sensor takes a finite amount of time to respond,  $t_r$ . In general, CO or smoke sensors have response times in the range of 30 to 60 s.

The total time that elapses until the fire is detected is the sum of these individual times. For CO, this detection time,  $(t_D)_{CO}$ , is

$$(t_D)_{CO} = (t_A)_{CO} + \frac{1}{2} \left[ \frac{\ell_s}{60 v_o} \right] + t_R, \quad (19)$$

while for smoke, this detection time,  $(t_D)_D$ , is

$$(t_D)_D = (t_A)_D + \frac{1}{2} \left[ \frac{\ell_s}{60 v_o} \right] + t_R, \quad (20)$$

for sensors located along a belt entry at some specified  $\ell_s$ .

For sensors near the belt drive area, the times to detect a fire are given by

$$(t_D)_{CO} = (t_A)_{CO} + (0.5/v_o) + t_R, \quad (21)$$

$$\text{and} \quad (t_D)_D = (t_A)_D + (0.5/v_o) + t_R. \quad (22)$$

For fire detection along conveyor belt entries downstream of the separately protected belt drive area, the detection times at low **air** velocities are limited by the transport time of the CO or smoke to the sensor. At higher **air** velocities, detection times are limited by the time it takes to produce alarm levels of CO and smoke owing to the lower production rates of CO and smoke (see figures 3 and 4) and to greater **dilution** at the higher airflows.

### SENSOR SPACINGS AND ALARM THRESHOLDS

Both the spacing and the alarm threshold used for a given sensor should be capable of satisfying some



minimum constraints. By using the data in tables 4 and 6, the testwide average time from flaming ignition of the coal until ignition of the belt occurs is 14.25 min. By using this information, the following constraint may be placed upon the use of belt entry fire detection systems and its impact evaluated: The system *must* detect a small, flaming coal fire within a time, measured from the moment of ignition of the coal fire, of 14.25 min or less.

By using this constraint and equations (11), (12), (18), and (19), a determination can be made, for either CO or smoke sensors, as to the spacings and alarm thresholds of those sensors in a belt entry as a function of entry air velocities and entry cross-sectional areas.

The results of this determination, assuming  $t_r = 1.0$  min, are shown in figures 7 and 8 for CO sensors and smoke sensors, respectively. Each of these figures is a nomograph that uses the belt entry cross-sectional area and air velocity to determine the sensor alarm levels for either 305-m (1,000-ft) or 610-m (2,000-ft) spacings. These are the maximum allowable spacings for CO and smoke sensors. In an actual situation, the spacing may be somewhat less, depending upon the total length of the

entry to be protected. These maximum spacings would be used only if the length of entry is an exact multiple of either 1,000 or 2,000. Further, if the belt entry contains more than one belt drive, the distance between any two belt drives would contain sensors at some specified spacing, while the distance from the second belt drive to the tailpiece would contain sensors, possibly at a different spacing, but not exceeding either 1,000 or 2,000 ft. (See the "Detector Spacing—an example" section.)

Each nomograph is actually a composite of two nomographs. The left-hand side is for maximum sensor spacings of 1,000 ft while the right-hand side is for maximum sensor spacings of 2,000 ft. In the nomograph for CO sensors shown in figure 7, the maximum alarm threshold for CO is limited to 10 ppm for sensors spaced at 1,000-ft intervals and 8 ppm for sensors spaced at 2,000-ft intervals.

Figure 8 is a duplicate of figure 7, except that the vertical alarm scales are in units of inverse meters of optical density. In figure 8, the  $0.044\text{-m}^{-1}$  value corresponds to a class 2 smoke detector and the  $0.022\text{-m}^{-1}$  value to a class 1 smoke sensor. The alarm scale is limited to a maximum

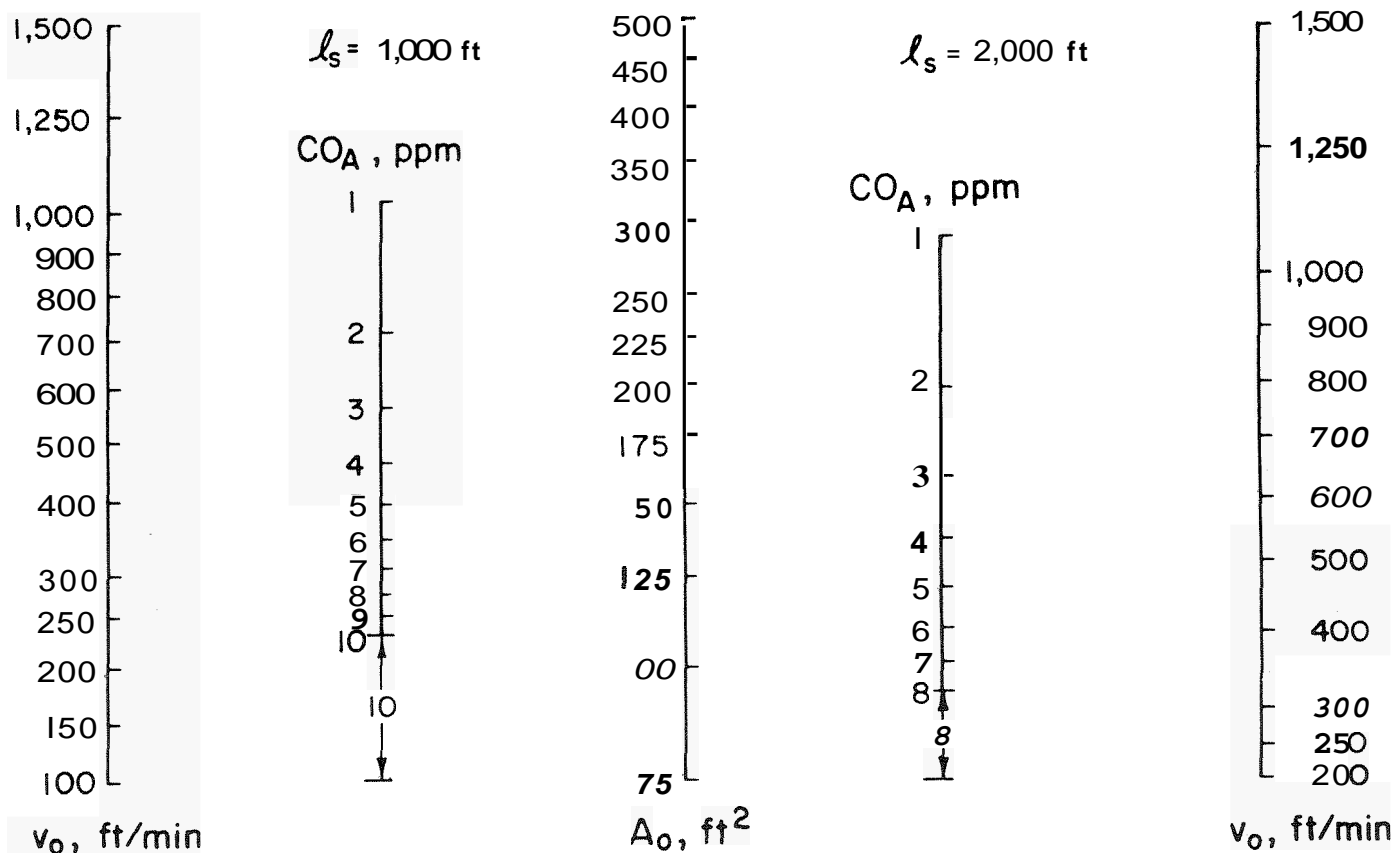


Figure 7.—Nomograph for CO sensor alarm thresholds and spacings.

value of  $0.044 \text{ m}^{-1}$ . The minimum value has been extended to include an alarm threshold of  $0.011 \text{ m}^{-1}$ , or **twice** as sensitive **as** a class 1 sensor. Reliable smoke sensors at **this** high level of sensitivity ( $0.011 \text{ m}^{-1}$ ) may or may not even be available, but this alarm level is included for completeness.

The manner in which these nomographs are to be used is **as** follows:

1. Determine the entry cross-sectional area,  $A_e$ , in square feet. It is recommended that the value for  $A_e$  be the geometric cross-sectional area, which is the product of entry height and width. (See Appendix D for modifications.)

2. Determine the entry **air** velocity,  $v_o$ , in feet per minute. The value used should be representative of the average velocity measured along the length of the entry. (See Appendix D for modifications.)

3. For 1,000-ft spacings, draw a straight line from the left-hand  $v_o$  scale to the value of  $A_e$ . This line intersects the CO alarm scale, or the smoke alarm scale, at the appropriate alarm level for this combination of  $v_o$  and  $A_e$ .

4. For 2,000-ft spacings, draw a straight line from the right-hand  $v_o$  scale to the value of  $A_e$ . This line intersects

the CO alarm scale, or the smoke alarm scale, at the appropriate alarm level for this combination of  $v_o$  and  $A_e$ .

5. When the indicated alarm level falls between **two** values, the lower value should be used.

### NOMOGRAPH USAGE—AN EXAMPLE

Mine "X" desires to reconfigure its ventilation system so that belt entry **air** may be used to ventilate a working section. The average cross-sectional area of the belt entry is  $100 \text{ ft}^2$ . With the new configuration, the average **air** velocity in the belt entry is expected to be  $400 \text{ ft/min}$ , but under certain conditions, the average **air** velocity may be as high as  $700 \text{ ft/min}$ . The mine operator proposes to use 5 ppm CO sensors spaced at intervals of 1,000 ft. Will **this** sensor alarm level and spacing be adequate?

From figure 7, the mine's entry cross section and average velocity of  $700 \text{ ft/min}$  yield an alarm level of 4 ppm for both 1,000-ft spacings and 2,000-ft spacings. At the average velocity of  $400 \text{ ft/min}$ , the nomograph yields an alarm level of 7 ppm for 1,000-ft spacings or 6 ppm for 2,000-ft spacings.

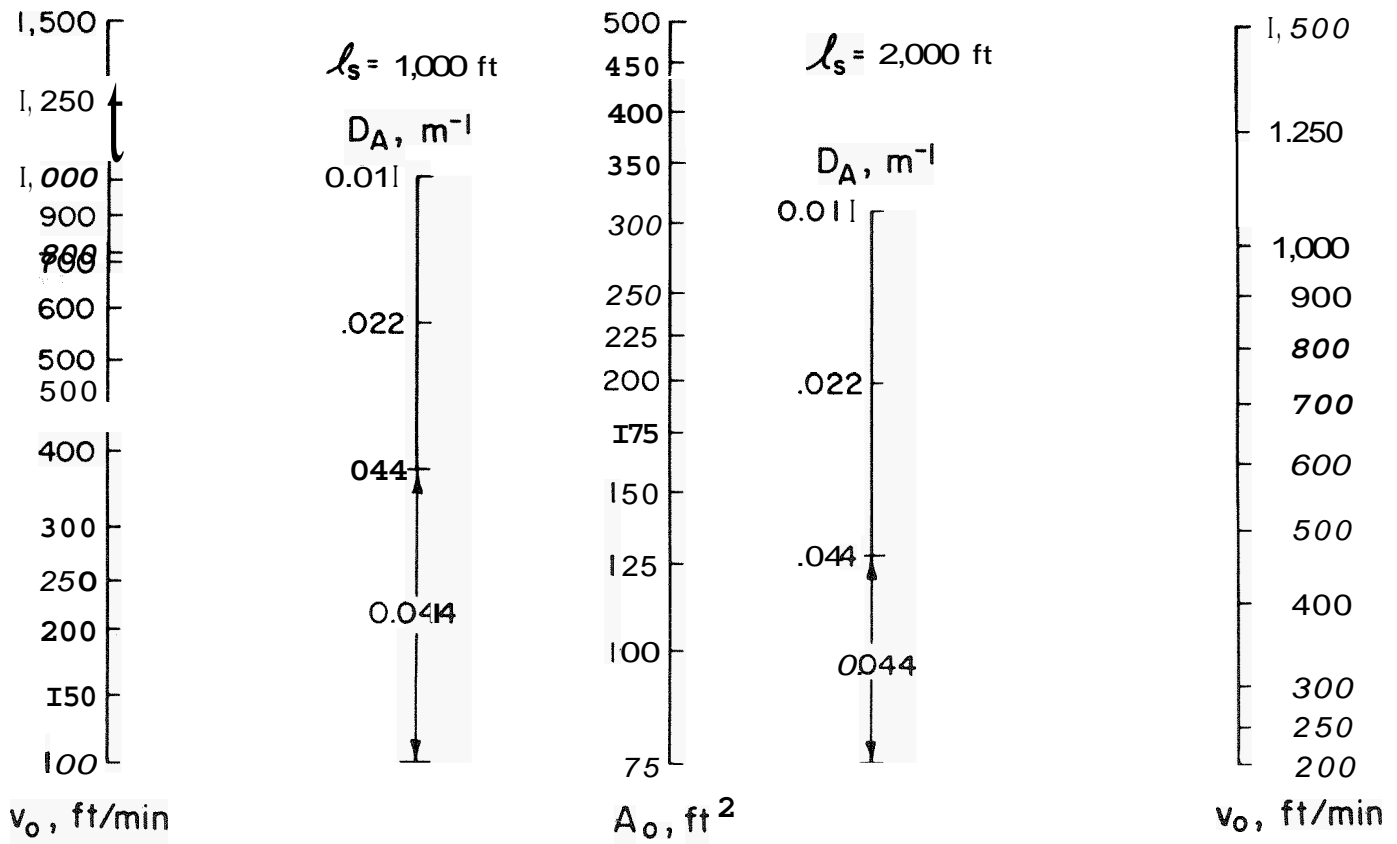


Figure 8.—Nomograph for smoke sensor alarm thresholds and spacings.

A similar analysis may be made for smoke sensors using figure 8. At either the average or maximum velocity, class 2 smoke sensors may be spaced at 2,000-ft intervals. This analysis indicates the following:

1. At the air velocity of 400 ft/min, 7 ppm CO sensors at 1,000 ft or 6 ppm CO sensors at 2,000-ft spacings may be used, or class 2 smoke sensors at 2,000-ft spacings;
2. At the air velocity of 700 ft/min, 4 ppm CO sensors at 2,000-ft spacings, or class 2 smoke sensors at 2,000 ft spacings would be required.

**DETECTOR SPACING—AN EXAMPLE**

The following belt entry is to be protected by CO sensors. The entry is 7,100 ft in length. Belt drive 1 is located 200 ft inby the headpiece. Belt drive 2 is located 3,800 ft inby the headpiece of belt drive 1. The tailpiece from belt drive 2 is located at a distance of 7,000 ft from the headpiece of belt drive 1. It was determined that CO sensors should be used at maximum spacings of 1,000 ft. The entry cross section is 100 ft<sup>2</sup> and the air velocity is 400 ft/min. From the previous example, the CO alarm level should be at 7 ppm. What are the actual spacings of the sensors along this entry?

The distance from drive 1 to drive 2 is 3,600 ft. Because drives will be protected separately, one sensor will be installed downstream of each drive at approximately 100 ft. Then, the first sensor will be located 300 ft

inby the headpiece. Another sensor will be located at 3,900 ft inby the headpiece. To determine the number of sensors and their spacings, divide 3,900 minus 300 by 1,000, which is 3.6. Any time this division falls between two integer values, the next highest integer value is the number of sensors required, with the last one at the end point (in this case, 100 ft past drive 2, or 3,900 ft). In between, sensors will be spaced at intervals defined by  $L_s = 3,600/4$ , or 900 ft.

The distance from the end of the entry (7,100 ft) to the sensor at 3,900 ft is 3,200 ft. This distance divided by 1,000 is 3.2, which means that four sensors are required along this length, but their spacing is 3,200/4, or 800 ft. The number of sensors and their locations are summarized in table 7.

**Table 7.—Location of sensors along example belt entry**

Sensor	Location, ft
1 . . . . .	300
2 . . . . .	1,200
3 . . . . .	2,100
4 . . . . .	3,000
5 . . . . .	3,900
6 . . . . .	4,700
7 . . . . .	5,500
8 . . . . .	6,300
9 . . . . .	7,100

**CONCLUSIONS**

The data have provided significant insight into the phenomena of fires that develop within conveyor belt entries. In general, both coal fires and subsequent belt fires before the onset of belt flame spread were found to grow at rates that increase with increasing air velocities. The rates of CO and smoke production were found to decrease as the air velocity increases.

For smoldering coal fires, the duration of the smoldering stage decreases as the air velocity increases, while the length of time from ignition of the coal until ignition of the belt increases as the air velocity increases. Once the SBR rubber belt ignites, the time to reach a stage of sustained flame spread decreases gradually as the air velocity increases. For the PVC belt, flame spread did not occur.

A constraint was proposed that may be used to define the conditions for use of proposed CO and smoke fire detection systems. For CO or smoke fire sensors, this constraint defines the sensor spacings and alarm thresholds for a range of air velocities and entry cross-sectional areas.

This constraint, derived from the data presented in this report and designed to approximate worst-case conditions for ignition of conveyor belting by a small precursor coal fire, defines the condition for sensor usage so that fire detection and alarm occurs just prior to ignition of conveyor belting.

It is extremely important to realize that if these data and subsequent constraints can be accepted as approximate worst-case conditions, then fires that develop via some other scenario will generally be detected earlier in their stage of development, thus providing more time for subsequent evacuations and control.

It is also extremely important to realize that this worst-case scenario can happen and that evacuation of personnel should be as rapid as possible owing to the short periods of time (10 to 20 min) that may be available until belt flame spread begins along with the untenable levels of combustion gases and smoke that result.

## REFERENCES

1. Lazzara, C. P., and F. J. Perzak. Conveyor Belt Flammability **Tests**: Comparison of Large-Scale Gallery and Laboratory-Scale Tunnel **Results**. Paper in Proceedings of the 23rd International Conference of Safety in Mines Research Institutes (Washington, DC, Sept. 11-15, 1989). BuMines OFR 2749, 1989, pp. 138-150; NTIS PB 89-225262/AS.
2. U.S. Code of Federal Regulations. Title 30—Mineral Resources; Chapter I—Mine Safety and Health Administration, Department of Labor, Subchapter B—Testing, Evaluation, and Approval of Mining Products; Part 18—Electric Motor Driven Mine Equipment and Accessories; Subpart C—Inspections and **Tests**; Section 18.65—Flame Test of Conveyor Belting and Hose, July 1, 1990, pp. 116-117.
3. Litton, C. D. Relationships Between Smoke and **Carbon Monoxide** and Their Implication **Toward** Improved Mine Fire Detection. Paper in Proceedings of the 23rd International Conference of Safety in Mines Research Institutes (Washington, DC, Sept. 11-15, 1989). BuMines OFR 2749, 1989, pp. 77-83; NTIS PB 89-225262/AS.
4. Egan, M. R. Coal Combustion in a Ventilated Tunnel. BuMines IC 9169, 1987, 13 pp.
5. Litton, C. D. Guidelines for Siting **Product-of-Combustion Fire Sensors** in Underground Mines. BuMines IC 8919, 1983, 13 pp.

**APPENDIX A.—HEAT-RELEASE RATES**

The fire heat-release rates may be calculated from measurements of the CO and CO<sub>2</sub> produced. When calculated on the basis of gas data, the resultant heat-release rate is assumed to be the total or actual heat-release rate.

The total heat-release rate is calculated from the expression

$$\dot{Q}_{\text{TOTAL}} = \left( \frac{H_C}{k_{\text{CO}_2}} \right) \cdot \dot{M}_{\text{CO}_2} + \frac{\dot{M}_{\text{CO}}}{k_{\text{CO}}} \quad (\text{A-1})$$

$\dot{M}_{\text{CO}_2}$  = generation rate of CO<sub>2</sub> from fire, g/s,

and  $\dot{M}_{\text{CO}}$  = generation rate of CO from fire, g/s.

$\dot{M}_{\text{CO}_2}$  and  $\dot{M}_{\text{CO}}$  are given by

$$\dot{M}_{\text{CO}_2} = 1.97 \cdot 10^{-3} v_o A_o \Delta \text{CO}_2, \quad (\text{A-2})$$

$$\text{and } \dot{M}_{\text{CO}} = 1.25 \cdot 10^{-3} v_o A_o \text{ACO}, \quad (\text{A-3})$$

where  $\Delta \text{CO}_2$  = CO<sub>2</sub> produced by fire, ppm,

$k_{\text{CO}_2}$  = stoichiometric yield of CO<sub>2</sub>, g/g,

= 3.67 • X<sub>c</sub>, where X<sub>c</sub> = mass fraction of carbon in fuel,

$k_{\text{CO}}$  = stoichiometric yield of CO, g/g,  
= 233 X<sub>c</sub>,

**Table A-1.—Values of H<sub>C</sub>, X<sub>c</sub>, k<sub>CO<sub>2</sub></sub>, and k<sub>CO</sub> for combustibles used in experiments**

Combustible	H <sub>C</sub> , kJ/g	X <sub>c</sub>	k <sub>CO<sub>2</sub></sub> , g/g	k <sub>CO</sub> , g/g
Sewickley Seam coal	30.0	0.712	2.61	1.66
R1 belt .....	36.8	.785	2.88	1.83
R11 belt .....	28.7	.638	2.34	1.49
P1 belt .....	23.4	.517	1.90	1.21

## APPENDIX B.—REPLACING POINT-TYPE HEAT SENSORS

There exists a particular situation regarding the use of CO or smoke sensors in place of point-type heat sensors along a belt entry. The U.S. Code of Federal Regulations, Title 30, **Part 75**, Subpart **L**, (in summary form) states that if the belt entry air velocity is 0.508 m/s (100 ft/min) or greater, point-type heat sensors must be spaced at intervals not to exceed 15.24 m (50 ft). If the belt entry air velocity is less than 0.508 m/s, point-type heat sensors may be spaced at intervals not to exceed 38.1 m (125 ft). The minimum alarm actuation temperature for a point-type heat sensor is 57.2° C (135° F). Other fire sensors (i.e., CO or smoke) may be used, provided they yield protection equivalent to that provided by point-type heat sensors.

The intent of appendix B is to demonstrate that CO or smoke fire sensors, when used at appropriate spacings and with appropriate alarm levels, **can** provide protection equivalent to, or better than, point-type heat sensors. In order to do this, it is assumed that if a CO or smoke fire detector system **can** be shown to be able to detect a developing fire in a time less than the time for a point-type heat sensor to detect the same developing fire, then the CO or smoke detection system satisfies the intended **definition** of equivalence.

Clearly a point-type heat sensor detects only open, flaming fires. Because of this, there exist two possible paths of fire development that **can** result in detection by point-type heat sensors. The first path is that of an open, flaming coal fire that increases in intensity until enough heat is produced to cause the point-type heat sensor to alarm without ignition of the conveyor belt. The second path is that of open, flaming coal fires that ignite the conveyor belt within the time frames observed in the tests reported here. The burning conveyor belt fire then increases in intensity until it is large enough to produce an alarm by the point-type heat sensor. Because this latter, second path of fire development was found to occur very rapidly in the tests conducted, only this fire scenario will be considered in the derivations that follow.

The expression that relates the fire intensity,  $\dot{Q}_T$ , thermal sensor spacing, and sensor alarm temperature,  $T_A$ , is given as follows (5):<sup>1</sup>

$$\dot{Q}_T = \rho_o C_o v_o A_o \left( \frac{T_A - T_o}{9} \right) \ell_T^{1.75 H/W}, \quad (\text{B-1})$$

where  $\rho_o$  = density of air,  $1.2010^3 \text{ g/m}^3$ ,

$$C_o = \text{heat capacity of air, } 1.088 \cdot 10^{-3} \frac{\text{kJ}}{\text{g} \cdot ^\circ\text{C}},$$

$$T_o = \text{ambient temperature, } 18.3^\circ \text{ C},$$

$$T_A = \text{heat sensor alarm temperature, } 57.2^\circ \text{ C},$$

$$H = \text{entry height, m},$$

$$W = \text{entry width, m},$$

and  $\ell_T$  = spacing between point-type heat sensors, m.

For  $v_o < 0.508 \text{ m/s}$ , the allowable spacing of thermal sensors is 38.1 m. A fire **can** occur anywhere between two sensors so that, on the average,  $\ell_T$  is one-half of 38.1 m or 19.05 m. For  $v_o \geq 0.508 \text{ m/s}$ ,  $\ell_T$  is set equal to one-half of 15.24 m or  $\ell_T = 7.62 \text{ m}$ .

In principle,  $H/W$  **can** have any value. However, it is limited for a specified value of  $\ell_T$  to some maximum value. This value is derived from the assumption that the fire size at thermal alarm **can** be no greater than the fire size predicted on the basis of complete mixing. It may be less, but it cannot be greater. The expression defining this constraint is

$$\rho_o C_o v_o A_o \left( \frac{T_A - T_o}{9} \right) \ell_T^{1.75 H/W} \leq \rho_o C_o v_o A_o (T_A - T_o), \quad (\text{B-2})$$

which reduces to

$$H/W \leq 0.57 \frac{\ln(9)}{\ln(\ell_T)}. \quad (\text{B-3})$$

$$\text{For } \ell_T = 19.05 \text{ m},$$

$$H/W \leq 0.425,$$

$$\text{and for } \ell_T = 7.62 \text{ m},$$

$$H/W \leq 0.62.$$

<sup>1</sup>Italic numbers in parentheses refer to items in the list of references preceding this appendix.

For a given value of  $A$ ,  $H$  and  $W$  have a range of values as long as  $HW = A$ . To address this range, it is assumed that the absolute minimum entry dimensions are  $H = 1.219 \text{ m}$  and  $W = 3.048 \text{ m}$  ( $4 \times 10 \text{ ft}$ ). The minimum value of  $H/W$ ,  $(H/W)_{\min}$ , at any other larger entry cross section is

$$(H/W)_{\min} = \frac{3.716}{A} \cdot 0.40 = 1.486/A_o. \quad (\text{B-4})$$

The maximum values of  $H/W$  at any larger entry cross section are defined above at the specified values of  $\ell_T$ . Because several possible values of  $H/W$  are allowed for any value of  $A$ , an average value is obtained by integrating over the range of values. This average value is then used in equation B-1 to estimate the average fire intensity necessary to produce thermal alarm for a given value of  $A$ .

Then, two calculations are made: The first calculation is the time required for a combined coal and belt fire to reach the specified value of  $\dot{Q}_T$  (equation B-1) at a specified air velocity; the second calculation is the time required for the fire to reach the maximum value of  $\dot{Q}_T$ , defined by the right-hand side of equation B-2. These times are called  $t_{\min}$  and  $t_{\max}$ , respectively, and represent the extremes that should be expected for point-type heat sensors to alarm.

The results of these computations for the cross-sectional area of the surface fire gallery ( $A_s = 7.53 \text{ m}^2$ )

as a function of the air velocity are shown in figure B-1. The measured thermal alarms at each air velocity are also shown. At air velocities of 0.76 and 1.52 m/s, the measured thermal alarm times tend to fall closer to the estimated minimum values, while at the air velocity of 4.06 m/s, the measured thermal alarm time corresponds to the maximum value. The reason for this is because of stratification of hot product gases that occurs at the lower velocities, while at the higher velocity, this stratified layer does not form.

The approximate minimum thermal alarm times that could be expected at air velocities of 0.254 and 0.508 m/s, as a function of entry cross section, are shown in figure B-2. It is emphasized in this figure that the minimum thermal alarm times are always greater than the average time to belt ignition of 14.25 min. It was this average time that was used as the constraint leading to figures 7 and 8; namely, that CO or smoke sensors shall detect a small, flaming coal fire in a time less than 14.25 min. Any combination of sensor alarm level and spacing obtained from the nomographs of figures 7 and 8 satisfies this constraint, and by definition, will detect the developing fire more rapidly than the estimated minimum time for point-type heat sensors to detect the same fire, as shown in figure B-2.

Consequently, any mine desiring to replace point-type heat sensors with either CO or smoke sensors should use the CO and smoke sensor nomographs in figures 7 and 8.

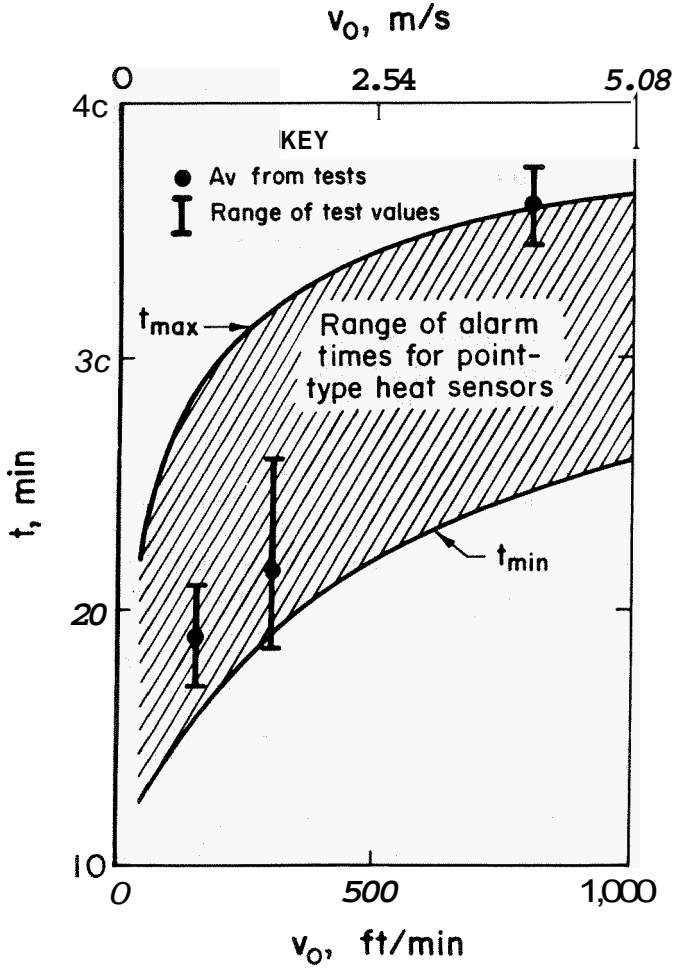


Figure B-1.—Thermal alarm times as function of air velocity for surface fire gallery tests. ( $A_0 = 7.53 \text{ m}^2$ .)

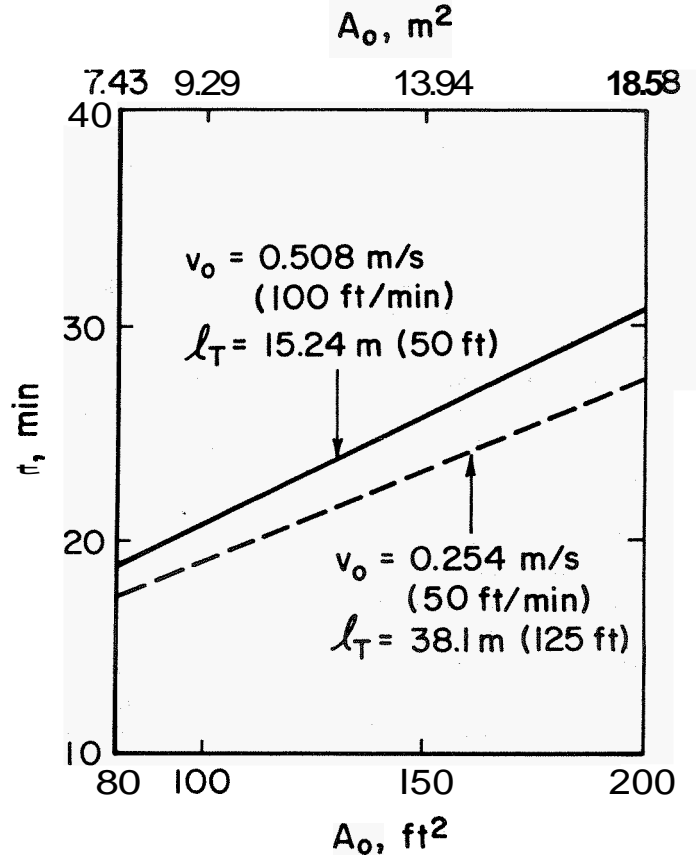


Figure B-2.—Thermal alarm times as function of entry cross section at velocities of 0.254 and 0.508 m/s. Average time to belt ignition for all tests was 14.25 min.



## APPENDIX C.—SMOKE OPTICAL DENSITY

The most widely measured smoke property is the light extinction coefficient,  $K$ . The physical basis for light extinction measurements is Bouguer-Lambert's law, which relates the intensity,  $I_{\lambda}$ , of an unattenuated incident **beam** of monochromatic light of wavelength  $\lambda$  and the intensity of light,  $I$ , transmitted through a path length of smoke,  $L$ , by the expression

$$I_{\lambda}/I_{\lambda}^0 = e^{-KL}, \quad (\text{C-1})$$

When this equation is expressed in terms of base 10,

$$I_{\lambda}/I_{\lambda}^0 = 10^{-D \cdot L}, \quad (\text{C-2})$$

where  $D$  = optical density,  $\text{m}^{-1}$ ,

and  $K = 2.303 \cdot D$ . (C-3)

Both  $K$  and  $D$  depend not only upon the wavelength of light, but **also** upon the **size** (diameter) of the smoke particles and their concentrations. When smoke is assumed to obscure visibility, the percent obscuration,  $O$ , is related to the transmission of light by the expression

$$O_u = 100 (1 - T). \quad (\text{C-4})$$

Here, the parameter,  $T$ , has been **used** for transmission because it represents some average **value** over **all** the wavelengths visible to the human eye **and also** because it represents some average value over **all** the particle diameters that form the smoke.

In this report, a smoke sensor with **an** alarm threshold of  $D_A = 0.044 \text{ m}^{-1}$  represents an obscuration of 9.6% over a 1.0-m path. **A** smoke sensor with **an** alarm threshold of  $D_A = 0.022 \text{ m}^{-1}$  represents an obscuration of **4.9%** over a 1.0-m path.

## APPENDIX D.—EFFECTIVE ENTRY CROSS SECTION AND AIR SPLITS

### CROSSCUTS

When fire sensors are installed in entries that contain crosscuts, the additional volume of entry space due to the crosscuts may increase the contaminant travel time between sensors and **also** dilute the contaminant concentrations. Both of these effects may seriously degrade the early **warning** capability of CO and smoke sensors. To offset **this** problem and retain the necessary early warning capability, the following procedures are recommended:

1. Determine the number of crosscuts and their approximate spacing along the entry to be protected. Divide the **number** of crosscuts,  $m$ , by their spacing,  $\ell_X$ , and designate the resulting number as  $N_X$ :

$$N_X = \frac{m}{\ell_X} \quad (\text{D-1})$$

For instance, if there are crosscuts on either side of the entry and they occur at 100-ft intervals, then  $m = 2$ ,  $\ell_X = 100$ , and  $N_X = 0.02$ . If there are crosscuts along only one side of the entry, then  $m = 1$  and  $N_X = 0.01$ .

2. Determine the average depth,  $d_X$ , of the crosscuts.

3. If 4, is the distance between fire sensors, then the total volume of space along the entry,  $V_E$ , with the crosscuts included is

$$V_E = \ell_S \cdot A_o + \ell_S \cdot N_X \cdot A_o \cdot d_X \quad (\text{D-2})$$

where it is assumed that the crosscuts have the same cross section as the entry,  $A_o$ . Thus,

$$\begin{aligned} V_E &= \ell_S \cdot A_o (1 + N_X \cdot d_X) \\ &= \ell_S \cdot A_o (1 + m \cdot d_X / \ell_X). \end{aligned} \quad (\text{D-3})$$

**Now** the straight-line distance between sensors remains the same and the net effect of the crosscuts is to increase the effective entry cross section,  $A_{EX}$  to a larger value given by

$$A_{EX} = A_o \left[ 1 + \frac{m \cdot d_X}{\ell_X} \right] \quad (\text{D-4})$$

When  $A_o$  is increased by using the expression given in equation D-4, the effects of crosscuts are overestimated.

Therefore, it is suggested that a more reasonable value for  $A_{EX}$  is given by

$$A_{EX} = A_o \left[ 1 + \frac{m \cdot d_X}{\ell_X} \right]^{1/2} \quad (\text{D-5})$$

This expression (equation D-5) is sufficient to account for both the increased travel time and dilution effects due to crosscuts. When figures 7 and 8 are used to determine sensor alarm levels, the value  $A_{EX}$ , rather than  $A_o$ , should be used.

For instance, if  $m = 2$ ,  $d_X = 25$  ft, and  $\ell_X = 100$  ft, then  $A_{EX} = (1.5)^{1/2} A_o = 1.22 A_o$ . If  $A_o = 100$  ft<sup>2</sup>, then to calculate the proper sensor alarm level at a given spacing,  $A_{EX} = 122$  ft<sup>2</sup> should be used. From figure 7, if the air velocity is 300 ft/min and the entry cross section is 100 ft<sup>2</sup>, then for 1,000-ft spacings the CO alarm level should be 9 ppm. However, including crosscuts, for which  $A_{EX} = A_o = 122$  ft<sup>2</sup>, a CO alarm level of 7 ppm for sensors spaced at 1,000-ft intervals is obtained from figure 7.

### PARALLEL ENTRIES

In some mines, two individual entries may exist that are not separated by stoppings. In these cases, the conveyor belt haulage system is usually located in one of the entries, but because **no** stoppings exist, the contaminants from a fire may be diluted by ventilating **air** from the parallel entry that does not contain the conveyor belt. To address this situation, the entry cross section,  $A_o$ , should be replaced by an effective entry cross section, which is the sum of the cross section of the individual entries.

For instance, if two entries have the same cross section, then the effective cross section,  $A_{EX}$  for determining sensor alarm levels is  $A_{EX} = 2 \cdot A_o$ . This is probably the most frequent situation. But if the entries have different cross sections  $A_1$  and  $A_2$ , then  $A_{EX} = A_1 + A_2$ .

As an example, if two of these parallel entries exist and are of equal cross section,  $A_o = 100$  ft<sup>2</sup>, then  $A_{EX} = 200$  ft<sup>2</sup> should be used for determining sensor alarm levels. From figure 7, if  $v_o = 150$  ft/min and  $A_{EX} = 100$  ft<sup>2</sup>, 10-ppm alarm levels could be used for 1,000-ft spacings. **When**  $A_{EX} = A_o = 200$  ft<sup>2</sup> due to parallel entries, figure 7 indicates 6-ppm alarm level for 1,000-ft spacings.

### COMBINED CROSSCUTS AND PARALLEL ENTRIES

When parallel entries contain crosscuts, the crosscuts exist **on only** one rib of each entry **since** there are no stoppings between the two entries. In this situation,  $m = 1$  for each entry. The effective cross sections of each entry due to the crosscuts are

$$(A_{EX})_0 = \left[ 1.0 + \frac{d_{X1}}{\ell_{X1}} \right]^{1/2} \quad (D-6)$$

and  $(A_{EX})_1 = \left[ 1.0 + \frac{d_{X2}}{\ell_{X2}} \right]^{1/2} A_1$  (D-7)

For instance, if  $d_{X1} = d_{X2} = 25$  ft and  $\ell_{X1} = \ell_{X2} = 100$  ft, then  $(A_{EX})_0 = 1.12 A_0$  and  $(A_{EX})_1 = 1.12 A_1$ . The total net effective cross section,  $A$  is  $A = (A_{EX})_0 + (A_{EX})_1 = 1.12 (A_0 + A_1)$ .

In the above example, if  $A_0 = A_1 = 100$  ft<sup>2</sup> and contains crosscuts, then  $A = 224$  ft<sup>2</sup>. From figure 7, at

$v_0 = 150$  ft/min and  $A = 224$  ft<sup>2</sup>, a 6 ppm alarm level could be used at spacings of 1,000 ft.

### AIR SPLITS

An air split is defined as any junction along a belt entry where ventilating air is either diverted to another entry (thus reducing the air velocity) or ventilating air from another entry is diverted into the belt entry. For purposes of determining sensor alarm levels, the length of airway between any two air splits should be treated as a distinct entry.

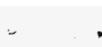
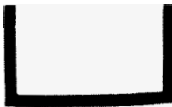
For instance, if  $A_0 = 125$  ft<sup>2</sup>, no parallel entries exist, the entry contains no crosscuts, and the airflow between two air splits is 200 ft/min, then from figure 7, at a spacing of 1,000 ft, the CO alarm level is 9 ppm. If, at the next air split, ventilating air is diverted to the belt entry from another entry, thus increasing the air velocity to 350 ft/min along the next section of entry, figure 7 would indicate that the CO sensor alarm level should be decreased to 6 ppm. The net effect of air splits is a change in the sensor alarm levels along a belt entry, based upon the changes in ventilation air velocity that occur because of the air splits.

## APPENDIX E.—LIST OF SYMBOLS

$A_{EP}$	total entry cross-sectional area including parallel entries, $m^2$	$\Delta t$	time from onset of smoldering coal to onset of flaming coal, min
$A_{EX}$	effective entry cross-sectional area when cross cuts are included, $m^2$	$\dot{G}_{CO}$	CO production rate, $\frac{ppm \cdot m^3}{s}$
$A_{EXP}$	total entry cross-sectional area when both parallel entries and crosscuts are included, $m^2$	$\dot{G}_D$	smoke production rate, $\frac{m^{-1} \cdot m^3}{s}$
$A_o$	nominal cross-sectional area of conveyor belt entry, $m^2$	$H$	entry height, m
$A_1$	nominal cross-sectional area of parallel entry, $m^2$	$H_C$	heat of combustion of coal or conveyor belt, $kJ/g$
$\alpha$	CO production rate constant, $\frac{ppm \cdot m^3}{s \cdot min}$	$H_{CO}$	heat of combustion of CO, $kJ/g$
$\alpha_{COAL}$	growth-rate parameter for coal fire, $kW/min$	$I$	smoke attenuated light intensity, W
$\alpha_{PVC}$	growth-rate parameter for PVC conveyor belt fire, $kW/min$	$I_o$	unattenuated light intensity, W
$\alpha_{SBR}$	growth-rate parameter for SBR conveyor belt fire, $kW/min$	$K$	light extinction coefficient, $m^{-1}$
$B_{CO}$	CO production constant, $\frac{ppm \cdot m^3}{kJ}$	$k_{CO}$	stoichiometric yield of CO, $g/g$
$B_D$	smoke production constant, $\frac{m^{-1} \cdot m^3}{kJ}$	$k_{CO_2}$	stoichiometric yield of $CO_2$ , $g/g$
$C_o$	heat capacity of air, $\frac{kJ}{g \cdot ^\circ C}$	$L$	path length of light, m
$CO_A$	CO sensor alarm threshold, ppm	$\ell_s$	CO or smoke sensor spacing, m
$D$	smoke optical density, $m^{-1}$	$\ell_T$	point-type heat sensor spacing, m
$D_A$	smoke sensor alarm threshold, $m^{-1}$	$\ell_x$	crosscut spacing, m
$d_x$	depth of crosscut, m	$\lambda$	wavelength of light, $\mu m$
$\Delta CO$	increase in CO due to fire, ppm	$\dot{M}_{CO}$	generation rate of CO, $g/s$
$\Delta CO_2$	increase in $CO_2$ due to fuel, ppm	$\dot{M}_{CO_2}$	generation rate of $CO_2$ , $g/s$
$\Delta \dot{G}_{CO}$	change in CO production rate during smoldering stage of coal fire, $\frac{ppm \cdot m^3}{s}$	$m$	number of crosscut in entry
		$N_x$	number of crosscuts per meter of entry length, $m^{-1}$
		$O_u$	light obscuration, dimensionless
		$\rho_o$	density of air, $g/m^3$

## APPENDIX E.—LIST OF SYMBOLS—Continued

$\dot{Q}_{\text{COAL}}$	heat-release rate of coal fire, kW	$(t_D)_{\text{CO}}$	time to detect fire by CO sensor downstream of fire, min.
$\dot{Q}_{\text{PVC}}$	heat-release rate of PVC conveyor belt fire, kW	$(t_D)_D$	time to detect fire by smoke sensor downstream of fire, min
$\dot{Q}_{\text{SBR}}$	heat-release rate of SBR conveyor belt fire, kW	$t_f$	average time that coal fire will burn before conveyor belt ignites, min.
$\dot{Q}_T$	heat-release rate of fire, kW	$t_{\text{MAX}}$	estimated maximum time for point-type heat sensor to alarm, min
$\dot{Q}_{\text{TOTAL}}$	heat-release rate of combined coal and conveyor belt fires, kW	$t_{\text{MIN}}$	estimated minimum time for point-type heat sensor to alarm, min
T	light transmission, dimensionless	$t_{\text{PEAK}}$	time to peak fire intensity, min
$T_A$	alarm temperature for point-type heat sensor, °C	$t_R$	response time of fire sensor, min
$T_o$	ambient temperature, °C	$t_s$	time coal fire smolders before flaming ignition, min
t	time, min	$t_t$	transport time of contaminants, min
$t_A$	sensor alarm time (general), min	$V_E$	entry volume, m <sup>3</sup>
$(t_A)_{\text{CO}}$	time required for coal fire to produce a given alarm level of CO, min	$v_o$	air velocity, m/s
$(t_A)_D$	time required for coal fire to produce a given alarm level of smoke, min	W	entry width, m
$t_{\text{BI}}$	time at which conveyor belt ignited minus time at which coal began to flame, min	$X_c$	carbon mass fraction, $\frac{\text{g of carbon}}{\text{g of fuel}}$
$t_{\text{BFS}}$	time at which conveyor belt flame spread began minus time at which coal began to flame, min		



U.S. Department of the Interior  
Bureau of Mines  
2401 E Street, N.W., MS #9800  
Washington, R.C. 20241-0001

AN EQUAL OPPORTUNITY EMPLOYER

**OFFICIAL BUSINESS**  
**PENALTY FOR PRIVATE USE-\$300**

